ANALYSIS AND DESIGN OF CONTROL SYSTEMS FOR AIRCRAFT AND MISSILES

by

K. W. Han 韓光渭

Associate Professor of the Institute of Electronics, Chiao-Tung University

SUMMARY: In this paper, control systems for aircraft and missiles are analyzed and designed using a "stability curve" method which is particularily suitable for testing stability and adjusting parameters for complex control systems. Design procedures are given along with examples.

I. GENERAL INTRODUCTION

Since the first successful flight of a powered aeroplane on 17th of December 1903, to control an aeroplane has been a challenging problem to most engineers. Although the autopilot systems have existed since 1912, many new problems have been arisen due to the advent of high performance aircraft. Jet aircraft and missile systems are getting more complex each day, the problems of testing stability and adjusting parameters to meet specifications become more severe than ever. Available methods for analysis and design are still limited to the conventional frequency response analysis,[1] and the root locus methods.[2] For some systems, the parameter plane and parameter space methods can be used,[3,4] but the number of adjustable parameters is limited and detailed characteristics of a system can not be obtained. Most control systems for aircraft and missiles are multiple loop with multiple adjustable parameters, so a new method capable of showing the effects of all adjustable parameters and of indicating absolute as well as relative stability would be desirable. The purpose of this paper is to present the "stability curve" method[5] which is capable of multiparameter analysis and design.

II. STABILITY CRITERION AND METHODS OF PREDICTING CHARACTERISTIC ROOTS

In this paper, methods of analysis and design are based upon a

stability criterion which has been proposed by the author[5]. A brief review is given in this section, and applications are presented in the next two sections.

Stability criterion: For a linear Nth order system to be stable, the necessary and sufficient conditions are that all the roots of the odd powered part (p_i) and even powered part (z_i) of its characteristic equation are on the imaginary axis of s-plane, and their absolute values are related as

$$P_0<z_1<p_1<z_2<p_2 \ldots . \tag{1}$$

where p_0 is at the origin of s-plane.

Proof: For an Nth order system, the characteristic equation can be written as

$$F(s)=\sum_{i=0}^{N} a_i s^i=F_e(s)+F_o(s)=0 \tag{2}$$

where $F_e(s)$ and $F_o(s)$ are the even powered and odd powered parts respectively.

After dividing $F_e(s)$ by $F_o(s)$, then

$$F_e(s)/F_o(s)=-1 \tag{3a}$$

which is a pro per form for plotting root loci.

From Eq.(2) a general form of Eq.$(3)_a$ can be written in expanded form as:

$$\frac{A(s^M+A_{M-2}s^{M-2}+\cdots A_4s^4+A_2s^4+A_0)}{s(s^Q+A_{Q-2}s^{Q-2}+\cdots A_5s^4+A_3s^2+A_1)}=-1 \tag{3b}$$

where $A=a_{N-1}$, $Q=M=N-1$ for odd values of N, $A=a_{N-1}^{-1}$, $Q=N-2$, $M=N$ for even values of N.

The numerator and denominator polynomials in Eq.$(3)_b$ contain even powered terms only, and it is well known that the only factors of such polynomials are conjugate imaginary factors, except for the possible case of two pairs of complex roots with identical imaginary parts but one pair having a real part which is the negative of the real part of the second pair. Before proceeding the two polynomials must be factored,

and for any combination of factors other than that of Eq.(1) the system is unstable.

When the poles and zeros of Eq.$(3)_b$ satisfy Eq.(1), the imaginary axis is the locus of phase angle $\phi = \pm(\frac{1}{2} \pm n)\pi$, where n is an integer. Thus no root loci can cross the imaginary axis. The angles of arrival and departure of the root loci at the singular points (poles and zeros on the imaginary axis) are simply $\pm m\pi$ where m $=1, 3, 5\cdots\cdots$. Thus all root loci are confined to the left half of the s-plane, and the system must be stable.

If the sequence of poles and zeros is other than specified by Eq.(1) at least one segment of root locus is entirely in the right half of the s-plane. which can be checked by the angles of arrival and departure of the loci at the singular points, and the system is unstable. If a pole identically equal to a zero, this defines a pair of imaginary roots, and the system is at the stability limit.

After the poles and zeros of Eq.(3) are available and the system is proved to be stable, the rood loci can be sketched. From these loci the characteristic roots can be predicted approximately.

Because of the alternating sequence of poles and zeros the root loci are "lobes" extending into the left half of s-plane. Each lobe contains one root for which the magnitude of ω_n is bounded (approximately) by the magnitudes of the pole and zero which terminate that segment of locus. The lobes are roughly semicircles so the maximum real part of the root is approximately $\sigma = \frac{1}{2}|\ P\text{-}z\ |$. For each such lobe the maximum available damping ratio (ρ) may be determined by constructing a radial line from the origin tangent to the lobe. For closer approximations to the root values it is noted that for small values of the gain constant A in Eq.$(3)_b$ the roots are near the poles, and for larger A the roots are near the zeros. For still closer approximation a point may be selected on a locus segment and the gain number evaluated to provide a reference point.

Using the proposed stability criterion, the analysis and design of control systems with multiple adjustable parameters becomes simply the problem of finding the real roots of $F_e(s)$ and $F_o(s)$. These ave called stability equations in a later part of this paper, and the curves which

represent the distributions of the real roots (z_i and p_i) are called stability curves.

III. ANALYSIS AND DESIGN OF AIRCRAFT CONTROL SYSTEMS

In this section, three control systems for aircraft are considered, and each one represents a different kind of application. The block diagrams of these systems are assumed available, and they are regarded as linear and time invariant.[2]

(A). Displacement autopilot.

The first system to be considered is a displacement autopilot of a jet transport flying at 600ft/sec and at 40,000 ft altitude. Its block diagram is given in Fig.1, where θ is the pitch angle, s_{rg} is the sensitivity of the rate gyro and S_{amp} is the gain of the main amplifier.[2] It is required to know the characteristics of this system under the adjustments of the rate gyro feedback and the main amplifier gain.

From Fig.1, let $K_1=s_{amp}$ and $K_2=S_{rg}$. The characteristic equation is

$$s^4+10.805s^3+(9.375+13.9K_2)s^2+$$
$$(13.25+4.25K_2+13.9K_1)s+4.25K_1=0 \qquad (4)$$

Let $y=s^2$ and $\eta=4.25K_1$, the stability equations are

$$y^2+(9.375+13.9K_2)y+\eta=0 \qquad (5)$$

$$y+0.393K_2+1.221+0.302\eta=0 \qquad (6)$$

The stability curves are plotted in Fig.2, in which for each value of η a vertical line can be drawn, a set of p_i' s and z_i' s can be found, and a set of root loci can be sketched, thus the effects of the adjustable parameters can be defined. For $K_2=1$, the following observations can be made:

(1). For $\eta=0$, using the pole and zero locations in Fig.2, the root loci can be sketched as in Fig.3, where the characteristic roots (r_i) can be predicted as indicated.

(2). From Fig.2, for larger values of η, the magnitudes of p_i and z_i are increased but z_2 is decreased, thus the frequency of r_1 and r_2 will be increased while their damping ratio is decreased.

(3). At $\eta=60$, the system is at its stability limit, and has a pair of pure imaginary characteristic roots at $\omega_n=4.46$.

Similar observations can be made for other values of K_2. In short, all the information needed for analysis and design can be obtained from the relative positions of the stability curves, and all the effects of the adjustable parameters can be determined.

(B). Pitch control system for longitudinal autopilot.

The block diagram of a pitch control system for longitudinal autopilot is given in Fig.4. The main problem is to make the system stable at high angle of attack, (i.e. to design an aircraft which has better performance), without producing instability at low angle of attack.

From Fig.4, let $K_1=S_{1g}$ and $K_2=S_{rg}$. The characteristic equation at low angle of attack, is

$$s^4+10.9s^3+(17+150K_2)s^2+(80+60K_2+150K_1)s+60K_1=0 \quad (7)$$

Let $\eta=60K_1$, the stability equations are

$$y^2+(17+150K_2)y+\eta=0 \quad (8)$$

$$y+(7.35+5.5K_2)+0.23\eta=0 \quad (9)$$

Eqs.(8) and (9) represent a family of parabolas and a family of straight lines with a constant slope, respectively.

At high angle of attack, the characteristic equation is

$$s^4+10.9s^3+(90K_2-2)s^2+(27K_2+90K_1-110)s+27K_1=0 \quad (10)$$

and the stability equations are

$$y^2+(90K_2-2)y+0.45\eta=0 \quad (11)$$

$$y+(2.475K_2-10.1)+0.138\eta=0 \quad (12)$$

For $K_2=0.5$, the stability curves for both high angle and low angle of attack are plotted in Fig.5, from which the following observations can be made:

(1). The upper limit of η is at 320, which places the system at its stability limit at low angle of attack; and the lower limit of η is at 60, which places the system at its stability limit at high angle of attack.

(2). At the lower limit of η, the system is well damped, except that the small characteristic roots near the origin of the s-plane may not be damped. For $\eta=100$, the root loci are plotted in Fig.6, where the characteristic roots are located approximately. For larger value of η, the

value of frequency (ω_n) will be increased while the damping ratio (ρ) is decreased.

(3). For the same value of η, increasing K_2 will increase the frequency, and the damping ratio will be reduced accordingly. In order to increase the upper limit of η the value of K_2 should be increased, but the lower limit of η is actually not affected by the adjustment of K_2.

(4). At low angle of attack the frequencies of the complex characteristic roots (r_1,r_2) are approximately equal to the average value of z_2 and p_1, because all the loci which contain r_1 and r_2 are terminated at z_2 and p_1. At high angle of attack, the frequencies of r_1 and r_2 are approximately equal to the average value of z_1 and p_1, which can be seen by sketching the root loci, (for $\eta=100$ see Fig.6).

In the commonly used design methods,[2] several root loci are required, and the general procedure is to analyze the inner loop first and then to design the outer loop. Since the information obtained from the inner loop can not guarantee the characteristics of the system, a method of trial and error must be used, and a computer simulation is usually required. But using the stability curve method, the stability characteristics of the system can be defined exactly from the relative positions of the stability curves, and all the characteristic roots, can be predicted approximately for all combinations of the adjustable parameters.

(C). Automatic beam guidance system.

The geometry and the block diagram of an automatic lateral beam guidance system are given in Figs.7 and 8. The effects of all the adjustable parameters and the design procedure will be considered.

From Fig.7, let $K_1=S_{e_c}$, $K_2=S_{\dot{\sigma}_z}$, $K_3=S_{v_z}$ and $K_4=S_{r_{rc}}$, the characteristic equation is

$$s^6+12.3s^5+(23+92K_4)s^4+92K_3s^3+\frac{92g}{V_T}K_2K_3s^2+\frac{92g}{R}K_1K_2K_3s+\frac{9.2}{R}K_1K_2K_3=0 \qquad (13)$$

Assume $V_T=440$ft/sec, $g=32.2$, and let $\alpha=297K_1K_2K_3/R$, $\beta=6.7K_2K_3$, Eq,(13) becomes

$$s^6+12.3s^5+(23+92K_4)s^4+92K_3s^3+\beta s^2+10\alpha s+\alpha=0 \qquad (14)$$

and the stability equations are

$$y^3+(23+92K_4)y^2+\beta y+\alpha=0 \tag{15}$$

$$y^2+7.49K_3+0.812\alpha=0 \tag{16}$$

Eq.(15) can be separated into two parts, such as[5]

$$\delta_{11}=y^3+(23+92K_4)y^2 \tag{17}$$

$$\delta_{12}=-\beta y-\alpha \tag{18}$$

Eqs.(17) and (18) represent a family of curves and a family of straight lines respectively, and their intersections are the real roots of Eq.(15). For several values of K_4, the results of Eq.(17) are plotted in Fig.9, which indicates that the upper limit of the frequency (ω_n) of the complex characteristic roots is decided by the value of K_4. For example, if K_4 is chosen at 0.564, the maximum value of ω_n for all values of the other adjustable parameters will be less than 8.65.

For having a clear view about how to use these stability equations and the related curves, the following design procedure is proposed.

Step 1. For a pair of desirable complex characteristic roots sketch a root locus and estimate the required upper and lower limits of frequency (ω_n) on the imaginary axis of s-plane.

Step 2. Select the value of K_4 according to the upper limit of ω_n.

Step 3. Select two roots from Eq.(16), such that the larger root (p_2) is the lower limit of ω_n, and the smaller one (p_1) is near the value of frequency which the other characteristic roots are desirable. Thus the value of α in Eq.(16) is found at $\alpha=p_1^2p_2^2/0.812$.

Step 4. From Eq.(18), using the value of α in Step 3, a straight line can be drawn which gives the most desirable intersection points (z_i^2's) with the curves represented by Eq.(17).

Step 5. Using the results in Steps 3 and 4, the root loci can be sketched, and the locations of the characteristic roots can be found.

For example, if the main purpose is to design a system which has a pair of characteristic roots near $\rho=0.5$ and $\omega_n=6$, and all the other roots are near the origin of the s-plane or have large and negative values, then from Step 1 the root locus is sketched in Fig.10, where the required upper and lower limits of frequency are found at 9 and 4.5 respectively.

Following Step 2, from Fig.9, the curve for K_4 is selected which gives a maximum upper limit of ω_n at 8.7 providing that the value of β in Eq.(18) is small.

For Step 3, the larger root (p_2) is at 4.5, which is decided by Step 1, and the smaller root (p_1) is selected at 0.7, thus the value of α is 12.2, which is indicated by point A in Fig.9_b.

According to Step 4, the dotted line (B) is drawn, and the values of z_i's are found, which indicate that the system is stable and all the characteristic roots are located near the desirable places.

For the final step, the root loci are plotted in Fig.10, where the locations of the complex characteristic roots (r_1, r_2) have been checked with a spirule.

For this system, the ratio of K_1/R can be regarded as a parameter which depends upon the value of α, thus the minimum value of R is decided by K_1.

While the operating range (R) is large, the value of α becomes small,it can be represented by the parallel motion of line B in Fig.9_b, which indicates that the system is stable when the range (R) becomes infinity.

To design a system with a pair of desirable characteristic roots can be accomplished by other methods.[3,6] The main contributions of the proposed method are that (1) all the effects of the adjustable parametrs can be considered separately; (2) all the characteristic roots can be predicted approximately while adjusting parameters; (3) for an Nth order system only two stability equations of equal or less than $^1/_2$Nth order need to be analyzed,and (4) all the analyses are analytical except the final sketch of the root loci which are all in a similar shape.

IV. ANALYSIS AND DESIGN OF MISSILE CONTROL SYSTEMS

Since the transfer functions of the control systems of missiles (rigid) are the same as that of aircrafts,[2] only one system, for roll stabilization, is considered in this section, and its block diagram is given in Fig.11. The main purpose is to find the effects of the lead network and the gain of the amplifier (s_{amp}).

From Fig.11 since the value of "c" is small for both aerodynamic

and ballistic missiles,[2] the system will be analyzed for the worst condition, i.e.c=0. The characteristic equation is

$$s^5+(84+b)s^4+(84b+2750)s^3 +2750bs^2+2750K_1+2750K_1a=0 \quad (19)$$

where $K_1=S_{amp}$. The stability equations are

$$y^2+\frac{2750b}{84+b}y+\frac{2750K_1a}{84+b}=0 \quad (20)$$

$$y^3+(84b+2750)y+2750K_1=0 \quad (21)$$

The stability curves are plotted in Fig.12, which indicates that for each set of values of K_1 and b there is an upper limit of "a" for stability. For example, if $K_1=100$ and b=30, the dotted ling (A) indicates that the maximum value of "a" is 16. Fig.12 also indicates that for each set of values of "a" ond "b" there is an upper limit of K_1. For. b=30 and a=2, the maximum value of K_1 is at 1150 Which is indicated by the dotted line (B).

In Fig.12_b, since the magnitude of p_2 is quite large, it can be predicted that a pair of characteristic roots with large frequency may exist. If this kind of characteristic roots are desirable, the difference between p_1 and z_2 should not be too small, otherwise a pair of complex characteristic roots decided by p_1 and z_2 (with lower frequency) will dominate the characteristics of this system. For a=2, b=30 and $K_1=100$ the results are given in Fig.13.

If the values of "a" and "b" are assumed equal, i.e. to eliminate the lead network, the stability curves indicate that the system is unstable for any value of K_1, which means that the compensation network is required.

CONCLUSIONS

In view of all the systems considered in this paper, it is apparent that the stability curve method is a powerful tool for the analysis and design of aircraft and missile control systems. By this method, all the effects of adjustable parameters can be represented in one plane, and the locations of all the characteristic roots can be predicted approximately for any combination of adjustable parameters.

REFERENCES

1. I. M Horowitz, "Synthesis of Feedback Systems," Academic Press, New York, N. Y., 1963.
2. J. H. Blakelock, "Automatic Control of Aircraft and Missiles," John Wiley and Sons, Inc., New York, 1965.
3. D. D. Siljak, "Analysis and Synthesis of Feedback Control Systems in The Parameter Plane, Part I. Linear Control Systems," IEEE Trans. Applications and Industry, Nov. 1964,
4. K. W. Han and G. J. Thaler, "Analysis and Design of Control Systems using Parameter Space Method," Paper submitted to IEEE in June, 1965.
5. K. W. Han," High Order System Analysis and Design using Root Locus Method," Science Bulletin of National Chiao-tung University. Vol. I,, No. I, Oct. 1965.
6. S. H. Liu and G. J. Thaler, "An Analytical Method for Analysis and Design of Control Systems," IEEE Trans. on Automatic Control, Jan. 1965.

LIST OF SYMBOLS

s	Laplace operator
p_i	root of odd part of characteristic equation (absolute value)
z_i	root of even part of characteristic equation (absolute value)
a_i	coefficient of characteristic equation
y, η, K_1, K_2, α, β	transformed variables
ω_n	natural frequency
ρ	damping ratio
F_e (s), F_o(s)	two parts of characteristic equation
δ_{11}, δ_{12}	two parts of a stability equation
δ_e	elevator deflection
θ	pitch angle
R	distance
S_{amp}	main amplifier gain
S_{rg}	sensitivety of rate gyro

S_{dg}	sensitivity of directional gyro
S_{vg}, S_{rg}	sensitivity of vertical gyro and roll rate gyro
S_c	gain of coupler
V_T	true airspeed
g	gravitational constant
$\dot{\theta}$	pitch rate
r_1	characteristic root
λ	angular error
d	lateral distance of the aircraft off course
ϕ	roll angle

LIST OF CAPTIONS

Fig. 1 Block diagram of a displacement autopilot of a jet transport.
Fig. 2 Stability curves of a displacement autopilot.
Fig. 3 Root loci of a displacement autopilot.
Fig. 4 Block diagram of a pitch control system for longitudinal autopilot.
Fig. 5 Stability curves of a control system for longitudinal antopilot.
Fig. 6 Root loci of a control system for longitudinal antopilot.
Fig. 7 Geometry of lateral beam guidance,
Fig. 8 Block diagram of a lateral beam guidance system.
Fig. 9 Stability curves of a lateral beam guidance system
(a) for large value of frequency
(b) for small value of frequency.
Fig.10 A sketch of the root loci for a lateral beam guidance system.
Fig.11 Block diagram of a missile roll stabilization control system.
Fig.12 Stability curves of a missile roll stabilization control system.
Fig.13 Root loci of a missile roll stabilization control system.

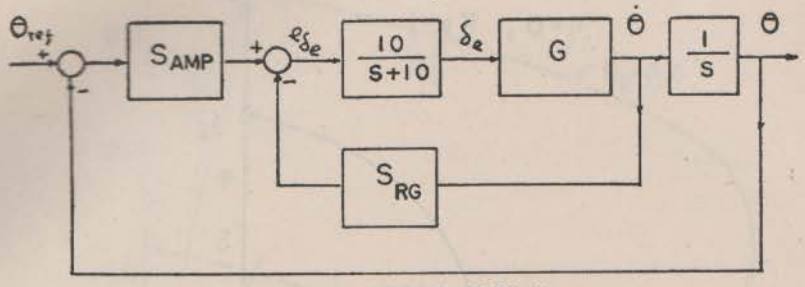
θref
+
-
SAMP
+
-
eδe
10
S+10
δe
G
θ̇
1
S
θ
SRG
G = 1.39(S+0.306) / S²+ 0.805S + 1.325

Fig.1

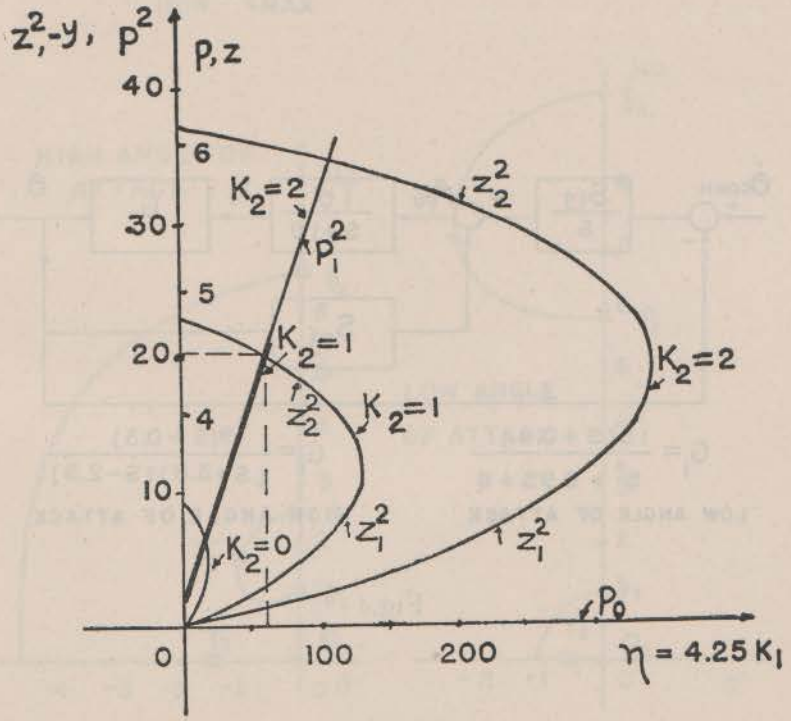
z₁²-y, p²
p,z
40
6
30
5
20
4
10
K₂=2
z₂²
p₁²
K₂=1
K₂=2
K₂=1
z₂²
K₂=0
z₁²
z₁²
P₀
0
100
200
η = 4.25 K₁

Fig.2

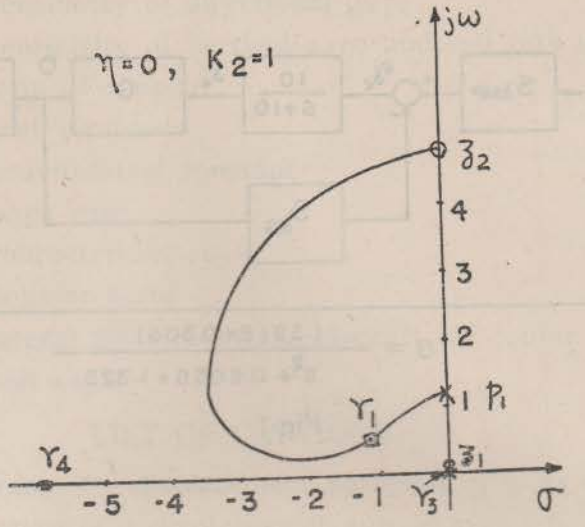
jω
η=0, K2=1
Z2
4
3
2
1
P1
Z1
Γ1
Γ4
Γ3
-5
-4
-3
-2
-1
σ

Fig 3

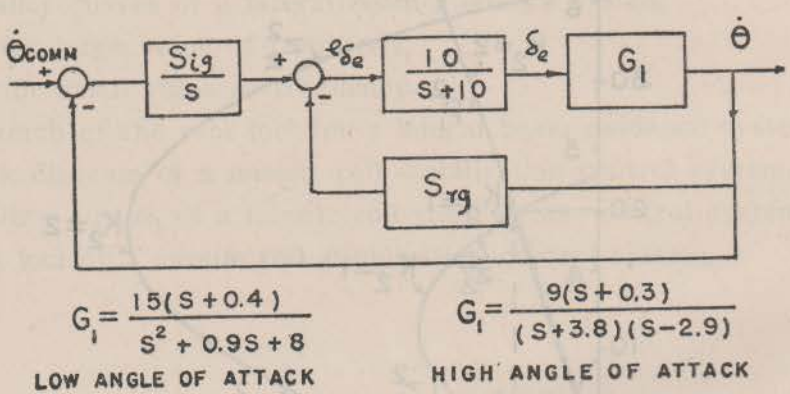
θ̇COMM
Sig
S
+
-
δe
10
S+10
δe
G1
θ̇
Srg
G1 = 15(S+0.4) / (S² + 0.9S + 8)
LOW ANGLE OF ATTACK
G1 = 9(S+0.3) / (S+3.8)(S-2.9)
HIGH ANGLE OF ATTACK

Fig.4

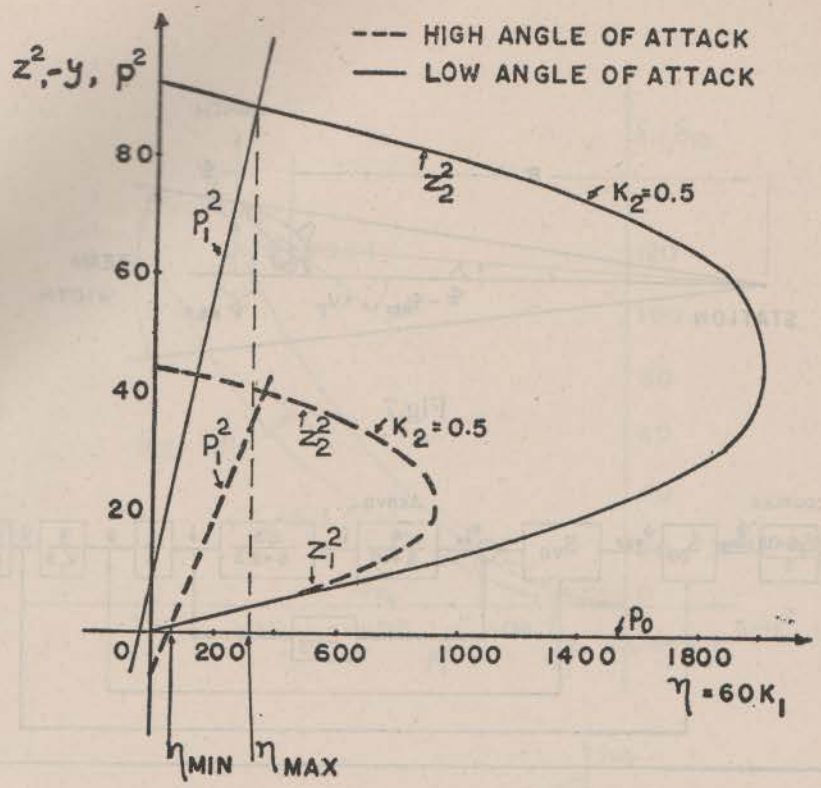
--- HIGH ANGLE OF ATTACK
—— LOW ANGLE OF ATTACK
$z^2, -y, p^2$
80
60
40
20
0
200
600
1000
1400
1800
$\eta = 60K_1$
P_0
z_2^2
$K_2=0.5$
p_1^2
$K_2=0.5$
z_1^2
η_{MIN}
η_{MAX}

Fig.5

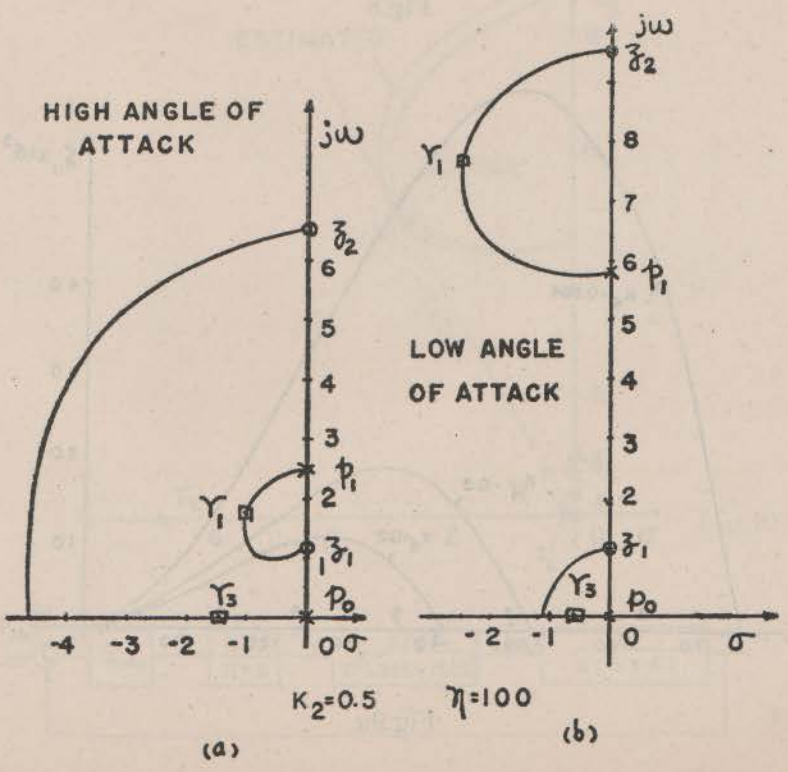
HIGH ANGLE OF ATTACK
jω
z_2
6
5
4
3
2
1
p_1
z_1
r_1
r_3
p_0
-4
-3
-2
-1
0 σ
$K_2=0.5$
(a)
jω
z_2
8
7
6
5
4
3
2
p_1
z_1
r_1
r_3
p_0
LOW ANGLE OF ATTACK
-2
-1
0
σ
η=100
(b)

Fig.6

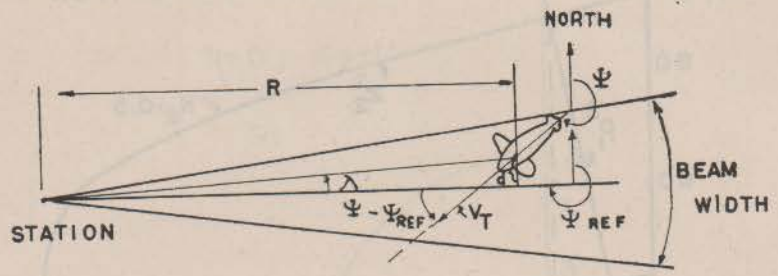

Fig.7

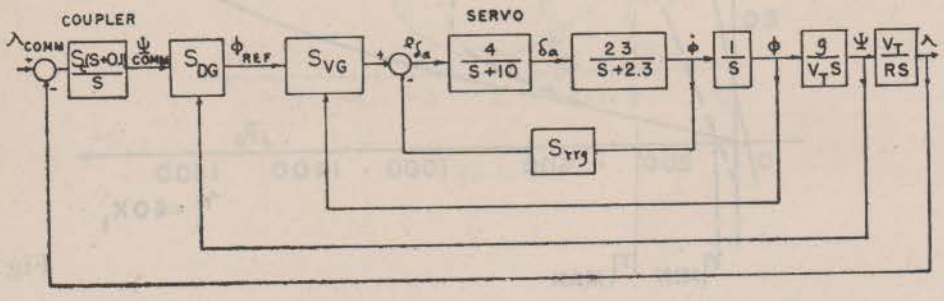

Fig.8

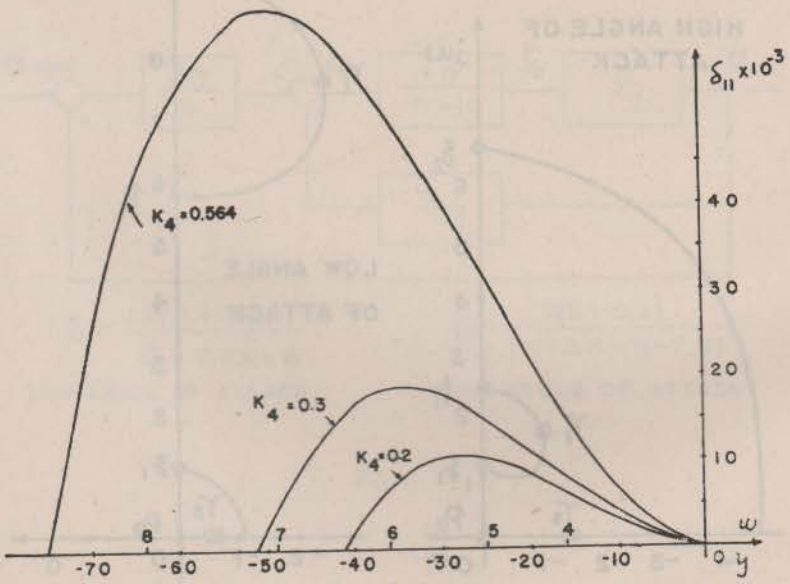

Fig.9a

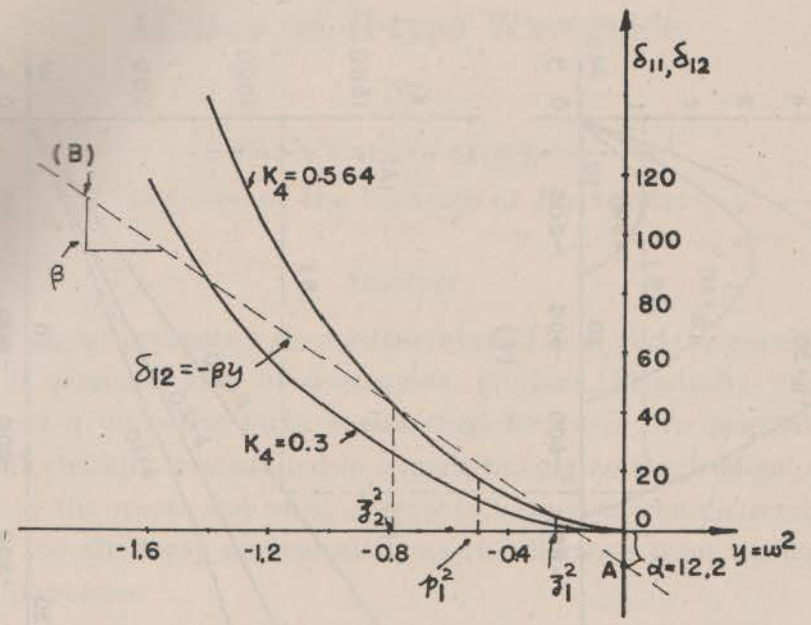

Fig.9b

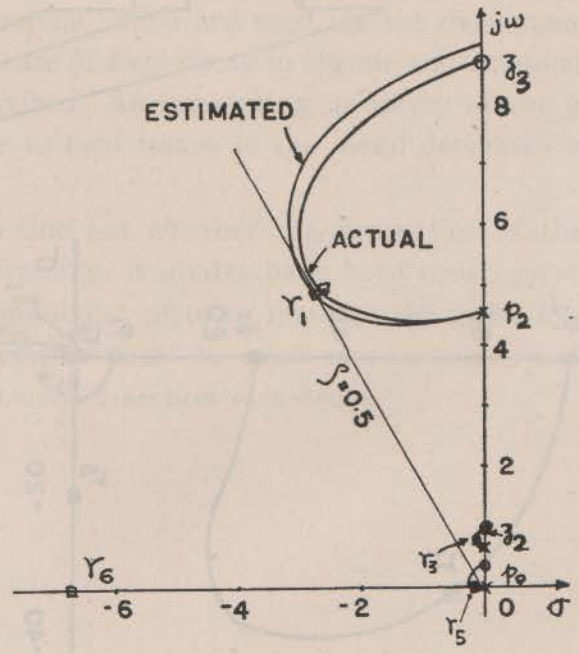

Fig.10

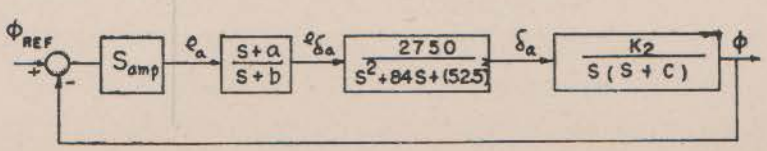

Fig.11

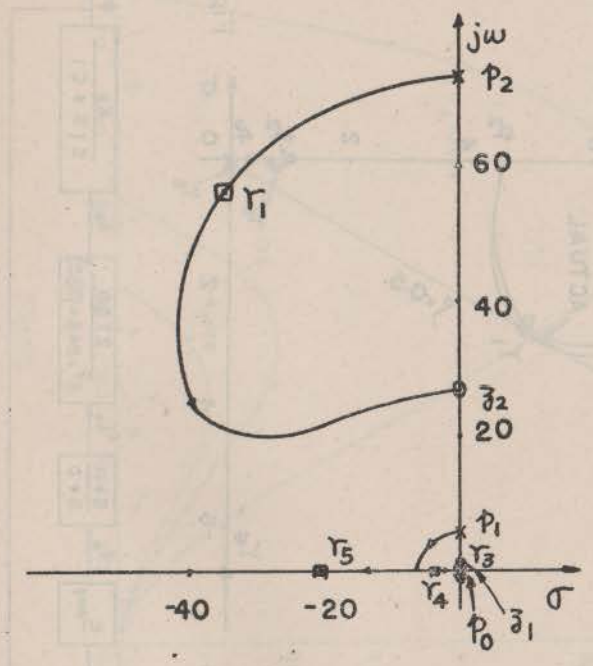
jω
P2
60
r1
40
z2
20
P1
r5
r3
r4
-40
-20
σ
P0
z1

Fig.13

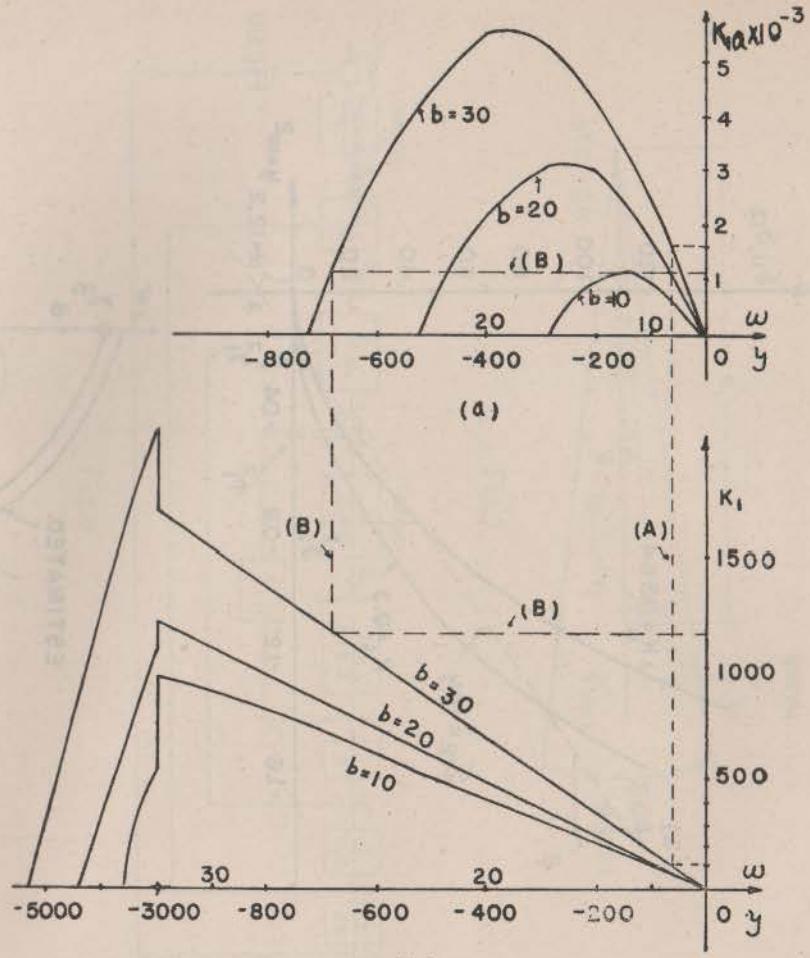
Kaα×10-3
5
4
3
2
1
b=30
b=20
(B)
b=10
20
10
ω
-800
-600
-400
-200
0
y
(a)
K1
(B)
(A)
1500
(B)
1000
b=30
b=20
b=10
500
30
20
ω
-5000
-3000
-800
-600
-400
-200
0
y
(b)

Fig.12